Engineering 13 (2022) 116–127

Contents lists available at ScienceDirect

Engineering

journal homepage: www.elsevier.com/locate/eng

Research
Green Chemical Engineering: Soft Matter—Review

Fabrication and Applications of Multi-Fluidic Electrospinning Multi-Structure Hollow and Core–Shell Nanofibers

Dianming Li [a,b], Guichu Yue [a], Shuai Li [a], Jing Liu [a], Huaike Li [a], Yuan Gao [a], Jingchong Liu [a], Lanlan Hou [a], Xiaofeng Liu [c], Zhimin Cui [a], Nü Wang [a,*], Jie Bai [c,*], Yong Zhao [a,*]

[a] Key Laboratory of Bioinspired Smart Interfacial Science and Technology of Ministry of Education, School of Chemistry, Beihang University, Beijing 100191, China
[b] School of Materials Science and Engineering, Lanzhou Jiaotong University, Lanzhou 730070, China
[c] College of Chemical Engineering, Inner Mongolia University of Technology, Hohhot 010051, China

ARTICLE INFO

Article history:
Received 30 July 2020
Revised 8 February 2021
Accepted 26 November 2021
Available online 29 April 2022

Keywords:
Electrospinning
Microfluidics
Multi-fluidic
Hollow structure
Nanofibers

ABSTRACT

Recently, electrospinning (ESP) has been widely used as a synthetic technology to prepare nanofibers with unique properties from various raw materials. The applications of functionalized nanofibers have gradually developed into one of the most exciting topics in the field of materials science. In this review, we focus on the preparation of multi-structure fibrous nanomaterials by means of multi-fluidic ESP and review the applications of multi-structure nanofibers in energy, catalysis, and biology. First, the working principle and process of ESP are introduced; then, we demonstrate how the microfluidic concept is combined with the ESP technique to the multi-fluidic ESP technique. Subsequently, the applications of multi-structure nanofibers in energy (Li^+/Na^+ batteries and Li–S batteries), hetero-catalysis, and biology (drug delivery and tissue engineering) are introduced. Finally, challenges and future directions in this emerging field are summarized.

1. Introduction

With the advent of nanotechnology at the end of the 20th century [1], an increasing amount of research has been done on nanofibers and their applications, mainly due to their unique properties such as adjustable chemical composition and engineered high porosity [2–5]. Among the diverse nanofiber-production methods that have been developed, electrospinning (ESP) is one of the simplest and most effective techniques for fabricating a wide range of one-dimensional (1D) nanomaterials from micron down to nanometer diameters [6–9]. ESP was invented in 1902, but it was not until the 1990s that researchers gradually discovered the great potential of ultrathin fiber materials [10]. It is notable that the number of publications in this area has been increasing rapidly over the past two decades (Fig. 1), due to the aforementioned advantages of this method. So far, ESP has been used to fabricate nanofibers of various materials, such as polymers, metallic compounds, carbon, or composite materials [11–13].

Since Loscertales et al. [14] prepared core–shell materials based on coaxial jets, nanofiber materials with various structures have been reported successively, including hollow structures [15–17], core–shell structures [18], multichannel structures [19], side-by-side structures [20,21], lotus-root-like structures [22], and vesicle structures [23]. In comparison with ordinary ESP fibers, multi-structure nanofibers exhibit some unique properties. As energy storage materials, conductive multi-structure nanofibers can provide a large amount of space at the micro/nanoscale, which effectively alleviates the volume expansion of the discharge products; there is also the possibility of further optimizing the various properties of nanofiber materials [24]. For catalysis, multi-structure nanofibers are beneficial for improving the spatial distribution of catalysts on the nanofibers, thereby exposing more active sites and providing a favorable catalytic environment [25]. In biological contexts, multi-structure nanofibers with optimized spatial distribution, surface properties, mechanical properties, and biodegradability have shown great potential in drug delivery and tissue engineering [26]. Thus far, multi-structure nanofiber materials have been widely used in energy, catalysis, biology, and many other fields.

* Corresponding authors.
E-mail addresses: wangn@buaa.edu.cn (N. Wang), baijie@imut.edu.cn (J. Bai), zhaoyong@buaa.edu.cn (Y. Zhao).

https://doi.org/10.1016/j.eng.2021.02.025

The concept of the coaxial ESP method that produces hollow or core–shell nanofibers is very similar to the microemulsion droplets generation concept by the co-flow microfluidic method. In terms of the device used, both methods require a coaxial spinneret that allows the fluid to mix in an orderly manner according to a specific proportion [27–30]; in terms of the fluid, both coaxial ESP and co-flow microfluidics require screening and optimization of the fluid's properties (e.g., surface tension, viscosity, solubility) so that the fluid can meet the requirements of the prepared materials [31,32]; and, in terms of products, both methods can prepare materials with a highly homogeneous structure and size [33,34]. In addition, fibers and emulsions with complex structures can be prepared via both methods by adjusting the techniques of ESP and microfluidics (e.g., device function, fluid parameters, injection rate) [35]. In the past two decades, both ESP and microfluidic technology have developed tremendously in the preparation of multi-structure materials. Designing a spinneret and introducing more kinds of fluids allow more complex structures to be prepared, as techniques that are useful in one method can be learned from the other method; thus, both methods exhibit broad application prospects [19,27].

In this review, we focus on the fabrication of various multi-structure nanofibers via multi-fluidic ESP and discuss their applications in energy, catalysis, and biology. We first briefly introduce the principle of ESP and the influencing factors in the ESP process. We then discuss the preparation of various multi-structure nanofibers—such as hollow, core–shell, multichannel, side-by-side, lotus-root-like, and vesicle nanofibers—by improving the ESP equipment and adjusting the polymer solution. Based on this discussion, we review the advances that have been achieved with multi-structure nanofibers in the fields of energy (Li^+/Na^+ batteries and Li–S batteries), catalysis, and biology (drug delivery and tissue engineering). Finally, we summarize the challenges and opportunities presented by multi-structure materials based on ESP in the future.

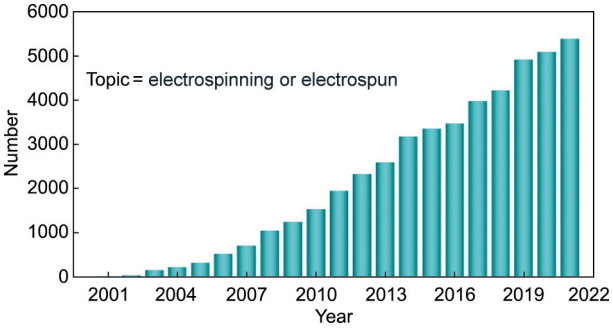

Fig. 1. Paper numbers using the keywords "electrospinning" and "electrospun" from 2000 to 2021. These results from Web of Science were available until December 2021.

2. The electrospinning technique

2.1. The principle of electrospinning

ESP is a facile technique to generate 1D fiber or zero-dimensional (0D) particle materials [36–40]. The ESP device consists of three components: a spinneret, high-voltage power, and a grounded conductive collector (Fig. 2(a)). The power can provide a voltage of several to tens of kilovolts between the collector and spinneret. The syringe first discharges the viscous polymer solution and/or suitable precursors (e.g., inorganic and carbon precursors) by gravity or a feeding pump. Under a high electric field, the meniscus polymer solution pendant drop is charged and experiences electrostatic forces. When the applied voltage is raised until the surface tension is lower than the electrostatic repulsive force, a conical-shaped jetting fluid (termed the "Taylor cone") is formed. In the jetting process, the Taylor cone fluid undergoes a whipping stretch process, which results in solidification of the melt or evaporation of the solvent; finally, solid nanofibers are formed on the collector (Fig. 2(b)) [41]. The jet can also be shrunk into globular individual particles by regulating the properties of the polymer solution, resulting in a large number of micro/nanoparticles (Fig. 2(c)) [19].

In general, many soluble polymers can be used to prepare fibers or micro/nanoparticles by adjusting the ESP parameters. The polymer properties (solubility, molecular weight, etc.), the polymer solution properties (concentration, viscosity, temperature, surface tension conductivity, etc.), the parameters of the ESP process (voltage, feed rate of soluble polymers, distribution of the electric field, type of collector, etc.), and the ambient parameters (humidity, temperature, gas atmosphere, air flow, etc.) play major roles during the preparation of the materials [42]. Researchers can adjust these parameters to achieve effective control of the structure (e.g., cylinder structure, flattened ribbon structure, bead-on-string structure, surface porous structure) and dimensions (nanoscale to microscale) [10,36].

2.2. Multi-structural materials

Since Loscertales et al. [14] optimized the combination of various polymer solutions and the design of a coaxial spinneret, a variety of multi-structure materials have been reported in succession.

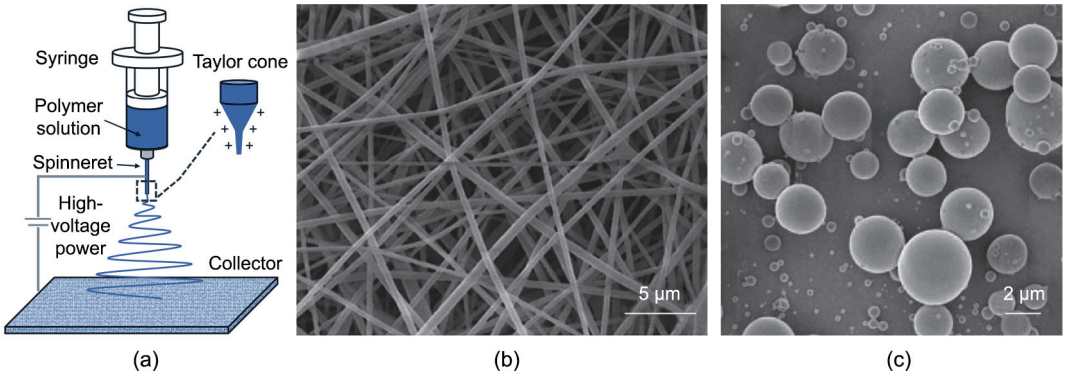

Fig. 2. (a) Conventional ESP equipment with three main parts: a spinneret, high-voltage power, and a grounded conducting collector. Typical ESP products obtained by controlling parameters include (b) fibers (via ESP) and (c) fine particles (via electrospray). (b) Reproduced from Ref. [41] with permission; (c) reproduced from Ref. [19] with permission.

This technology is now used by an increasing number of researchers to prepare multi-structure materials, such as hollow/core–shell nanofibers, multichannel nanofibers, multicavity microcapsules, side-by-side nanofibers, and more. In this review, we mainly focus on the fabrication of fibrous materials by ESP.

2.2.1. Hollow/core–shell nanofibers

Coaxial ESP differs from traditional ESP mainly in terms of the spinneret and polymer solution. The single spinneret used in traditional ESP is replaced by a coaxial spinneret in which two channels are connected to two syringes. The coaxial configuration of the spinneret can provide different pathways for inner and outer solutions. Under a high electric field, inner and outer solutions are charged, and a composite Taylor cone is formed. In the jetting process, the inner and outer solutions undergo a whipping stretch process at the same time, which results in solidification of the melt or evaporation of the solvent; finally, solid nanofibers are formed on the collector. The formation of a composite Taylor cone increases the difficulty of material preparation. When the viscosity of the two fluids is not well matched, a number of issues may ensue: A bead-like structure may form on the fiber skeleton; a small proportion of the shell fluid may fail to contain the core fluid; and two fluids with miscibility may be unable to achieve well-defined core–shell structures. Because the conductivity of the fluid will affect the charge distribution of the Taylor cone, it may not be possible to produce the core–shell structure fiber when the conductivity difference is large. Thus, in comparison with traditional ESP, additional considerations of the miscibility and conductivities between the core and shell solutions are critical for the successful production of hollow/core–shell nanofibers [1,43].

As shown in Fig. 3(a) [44], the composite spinneret is composed of two coaxial spinnerets. When spinning, heavy mineral oil is ejected from the internal spinneret and an ethanol solution containing polyvinyl pyrrolidone (PVP) and Ti(O*i*Pr)$_4$ is ejected from the external spinneret [44]. Uniform hollow nanofibers can be directly fabricated through this approach (Figs. 3(b) and (c)). This technology provides new thinking for the fabrication of hollow/core–shell nanofibers. After the development of the composite spinneret, coaxial ESP has been further developed for more than ten years [43,45,46]. An increasing number of polymer solutions are being developed as the precursors of fibers in order to expand the range of applications [47]. Alternatively, hollow/core–shell nanofibers with complex structures can be prepared by adding templates to the spinning solution to improve the performance in the fields of catalysis or energy [48].

Hollow/core–shell nanofibers can also be prepared by means of traditional ESP followed by heat treatment [12,37]. Yoon et al. [49] reported an approach for preparing efficient bifunctional electrocatalysts by utilizing ESP and calcination. As shown in Fig. 3(d) [49], sufficient time and appropriate temperature during the heat treatment caused [Ru–O$_x$] to preferentially aggregate in the inner region and caused the outer [Ru–O$_x$] to continuously diffuse into the interior. Finally, RuO_2/Mn_2O_3 nanofibers were obtained (Fig. 3(e)). This work opens up a simple way to fabricate various metal oxide hollow nanofibers using ESP technology.

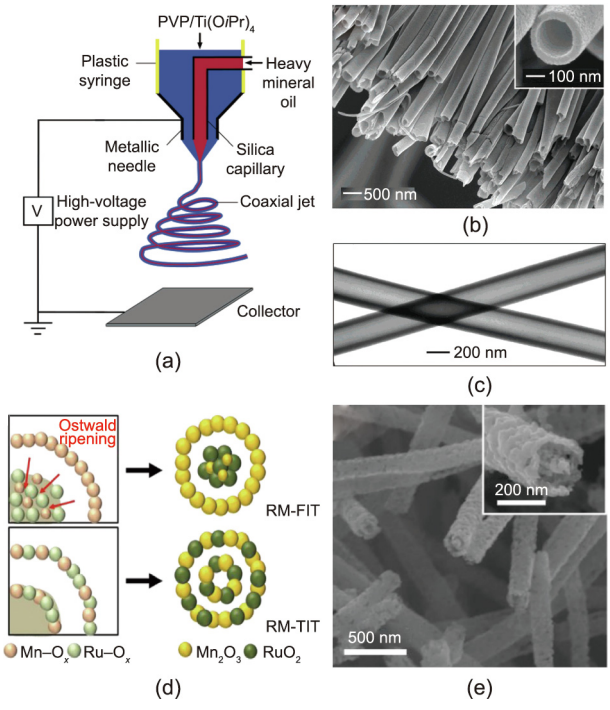

Fig. 3. (a) Schematic illustration of coaxial ESP (PVP: polyvinyl pyrrolidone). (b) Scanning electron microscope (SEM) and (c) transmission electron microscope (TEM) images of the hollow nanofibers. (d) Formation diagram of RuO_2/Mn_2O_3 fiber-in-tube (RM-FIT) and RuO_2/Mn_2O_3 tube-in-tube (RM-TIT). (e) SEM images of RM-FIT. (a–c) Reproduced from Ref. [44] with permission; (d, e) reproduced from Ref. [49] with permission.

2.2.2. Multichannel nanofibers and multicavity micro/nanoparticles

Multichannel nanofibers and multicavity microcapsules are typical structures prepared by multi-fluidic ESP. Multichannel and multicavity materials have attracted interest due to their unique applications [3,50]. Confronted with the huge challenge of producing multichannel tubular structures and multicavity microcapsule structures on a micro/nanometer scale, Zhao et al. [51] proposed a solution using multi-fluidic ESP. In Fig. 4(a) [51], the preparation of three-channel tubular fibers is demonstrated as an example. The researchers embedded three spinnerets that distributed at the vertices of an equilateral triangle. After the ESP process, fibers were accumulated on the collector. By decomposing the organic components in the fibers through heat treatment, three-channel TiO_2 tubes were obtained (Fig. 4(b)) [51].

The design idea of the spinneret used to obtain multicavity microcapsules is the same as that used for the above multichannel nanofibers (Fig. 4(c)) [19]. The viscoelasticity of the spray solution is much lower than that of the spinning solution, such that it is unable to sustain a stable thin liquid thread. As a result, the solution jet breaks up into numerous tiny droplets. The as-prepared particles exhibited spherical morphology, and the two core components were suppressed into individual compartments free of contact (Fig. 4(d)) [19].

Based on this concept, fibers with more channels and microcapsules with more components can be made by designing the configuration of the spinneret. If more channels and core components are necessary, the corresponding number of inner needles are inserted into the outer needle in a certain spatial position, and each needle is fed with core fluid (Figs. 4(e)–(l)) [19,51]. This method represents the early use of ESP technology to prepare multichannel nanofibers and multicavity microcapsules; it provides new thinking on how to prepare materials with complex structures.

2.2.3. Other multi-structure materials

In addition to the aforementioned structures, other typical structures, such as side-by-side structures, vesicle structures, and lotus-root-like structures, can be prepared by regulating the properties of the polymer solution and designing an appropriate spinneret.

Side-by-side nanofibers have recently attracted research attention because they have different exposed surfaces with different

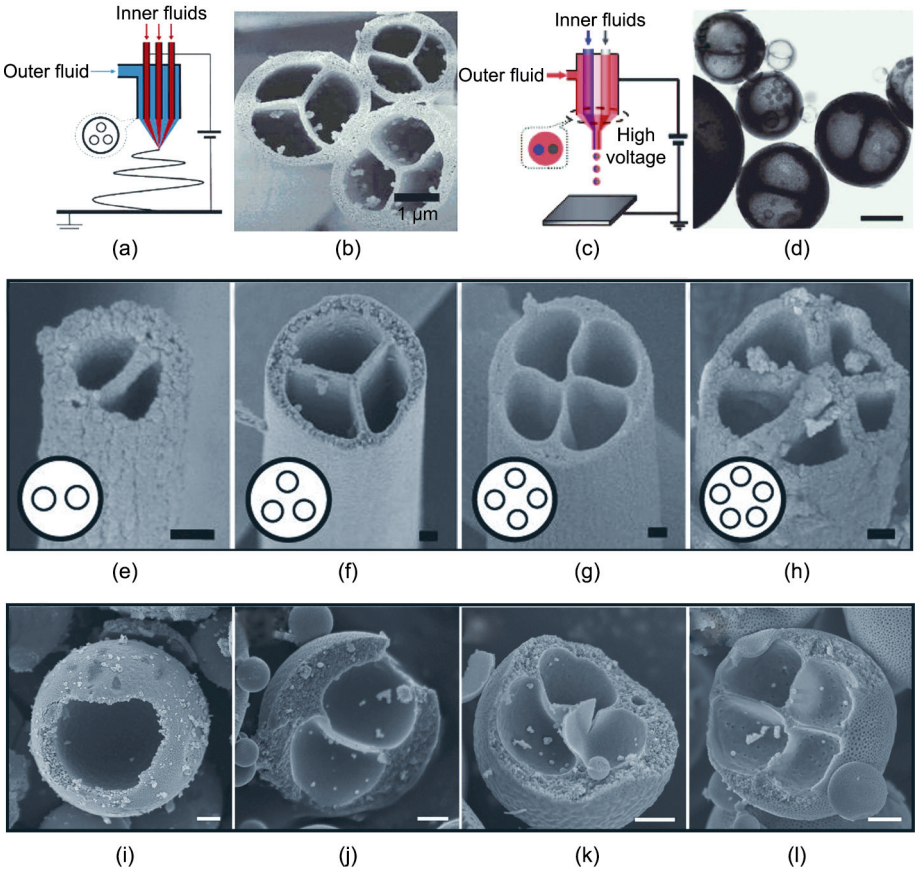

Fig. 4. (a) Schematic diagram of the multi-fluidic ESP process. (b) SEM image of multichannel nanofibers. (c) Schematic diagram of the multi-fluidic electrospray process. (d) TEM image of multicavity microcapsules (scale bar: 1 μm). (e–h) SEM images of fibers with different channel numbers (scale bars: 100 nm). (i–l) SEM images of microcapsules with different cavity numbers, ranging from one to four cavities (scale bar: 500 nm). (a, b, e–h) Reproduced from Ref. [51] with permission; (c, d, i–l) reproduced from Ref. [19] with permission.

components on the two opposite sides [21,52,53]. In 2005, Roh et al. [54] demonstrated the design of polymer particles with two phases. These particles, which were composed of two kinds of polymer, were prepared using a parallel spinneret. Inspired by this work, an increasing number of researchers are improving the ESP equipment to prepare side-by-side nanofibers. Figs. 5(a) and (b) [55] show a confocal laser scanning microscopy (CLSM) image of bicompartmental nanofibers with fluorescein and Nile red fluorescence signals. The CLSM image indicates that both compartments maintained fibrous structures, and distinct interfaces are observed. This side-by-side ESP approach, when applied to different polymer solutions, makes it possible to produce homogeneous biphasic nanofibers by regulating the rheological properties of polymer solutions (including complex viscosity and surface tension).

Vesicle nanofibers prepared by means of emulsion ESP are widely used in drug delivery systems and as electrode materials. Emulsion ESP has the same principles as common ESP, except for an emulsified spinning solution (Fig. 5(c)) [23]. This emulsion is a dispersion system in which a fluid is dispersed into numerous tiny droplets within another continuous immiscible fluid. During the ESP process, the viscosity of the continuous phase increases rapidly with the volatilization of the solvent. Finally, the dispersed-phase droplets deform into a columnar shape under the action of the viscosity shearing gradient, forming fibers with a vesicle structure [56]. Several parameters, including the electric field strength, type of emulsion, surface tension, solution flow rate, and conductivity of the solution, can affect the structure of vesicle fibers; therefore, fibers with wide application prospects can be prepared by controlling these parameters.

Lotus-root-like nanofibers are another typical multi-structure material prepared by means of ESP. In a typical procedure, two incompatible polymer precursors (e.g., the mixture of polystyrene (PS)/polyacrylonitrile (PAN)) are dissolved to form a stable mixed solution in which the two polymers are in a microphase separation state. During the ESP process, the dispersed phase is extruded and stretched into nanoscale wires; next, lotus-root-like nano-channels are generated after selective pyrolysis or a dissolution process, as shown in Fig. 5(d) [57]. The channel structures of the lotus-root-like nanofibers can be readily changed by controlling the ratio of the dispersed-phase polymers [22].

In conclusion, multi-structure fibrous materials such as hollow fibers, core–shell fibers, multichannel fibers, multicavity microcapsules, side-by-side fibers, vesicle fibers, and lotus-root-like fibers can be controllably prepared by means of the multi-fluidic ESP method. At present, ESP technology is one of the simplest methods to prepare these multi-structure materials and thus expands the scope of application of such materials.

3. Applications of multi-structure fibrous materials

Due to their various structures, adjustable chemical composition, and high surface area, multi-structure nanofibers have been used in many fields [58]. Multi-structure nanofibers can provide a large amount of space at the micro/nanoscale to improve the

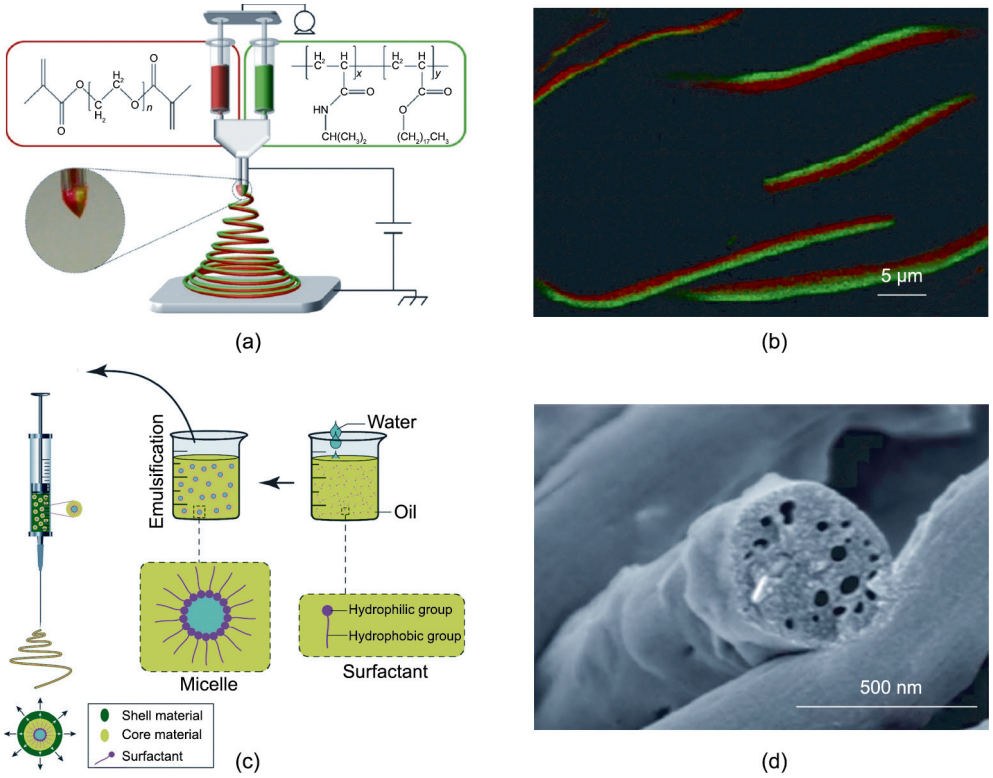

Fig. 5. (a) Schematic diagram of a side-by-side ESP process. (b) Confocal laser scanning microscopy (CLSM) image of the side-by-side nanofibers. (c) Schematic diagram of an emulsion ESP process. (d) SEM image of lotus-root-like nanofibers. (a, b) Reproduced from Ref. [55] with permission; (c) reproduced from Ref. [23] with permission; (d) reproduced from Ref. [57] with permission.

performance of electrode materials. In addition, the many types of nanofiber structures are beneficial for improving the space utilization efficiency in order to increase the contact opportunities between reactants and active sites in catalytic reaction. Moreover, multi-structure nanofibers can easily be designed as materials with porous, controllable degradation and excellent mechanical properties for drug delivery and tissue engineering. To date, many researchers have been devoted to achieving successful applications in the areas of energy, catalysis, and biology [40,59,60].

3.1. Nanofiber application in energy-related applications

As an integral part of functional materials, multi-structure nanofibers with void space offer a large electrode–electrolyte contact area for fast diffusion and accommodate the nonnegligible volume variation in charging/discharging processes. With sulfur hosts, the void space of multi-structure nanofibers is beneficial for the loading of sulfur. These nanofibers have now been demonstrated to have enormous potential for advanced energy storage and conversion technologies, such as Li^+/Na^+ batteries and Li–S batteries.

3.1.1. Li^+/Na^+ batteries

Recently, Li^+ batteries (LIBs) have been regarded as one of the most useful energy sources for electric vehicles and mobile electric devices [61–67]. Na^+ batteries (SIBs) have also attracted attention due to their key advantages, which include abundant natural resources and low cost [68]. As electrodes for LIBs/SIBs, active nanomaterials should have facile strain relaxation, a short ion insertion/extraction distance, and an appropriate surface-to-volume area to come into contact with the electrolyte [4]. However, because of their high activity and surface energy, nanomaterials tend to aggregate, which reduces the contact area between the conductive additives and the active materials [10]. The multi-structure materials prepared by ESP, such as core–shell nanofibers, hollow nanofibers, vesicle nanofibers, and lotus-root-like nanofibers, ensure effective contact even if there is a small amount of self-aggregation. Therefore, multi-structure nanofibers are one of the most favorable electrode materials [69–75].

Hwang et al. [76] developed an ESP process to prepare core–shell nanofiber electrodes (Fig. 6(a)). Commercial silicon (Si) nanoparticles were wrapped in the core by a carbon shell, as shown in Fig. 6(b). The unique core–shell structure alleviated many of the problems of a Si anode during charge and discharge, such as unstable contact between the Si nanoparticles and the conductive carbon, and the vulnerability of the solid-electrolyte interphase. The Si nanoparticles at C nanofibers exhibited excellent performance, with a gravimetric capacity as high as 1384 $mA{\cdot}h{\cdot}g^{-1}$, a 5 min discharging rate capability while retaining 721 $mA{\cdot}h{\cdot}g^{-1}$, and a cycle life of 100 cycles with almost no capacity loss (Fig. 6(c)) [76]. The ESP core–shell nanofiber provides a new way of design that addresses the volume expansion of LIB electrodes.

Li et al. [77] prepared $CaSnO_3$ nanotubes (CSO-NTs) by means of a facile ESP method followed by calcination (Figs. 6(d) and (e)). The scanning electron microscope (SEM) image in Fig. 6(e) clearly shows that the CSO-NT has a hollow structure with rough inside and outside surfaces. When used as anode materials, CSO-NTs exhibited good cyclic stability. Wang et al. [56] fabricated highly Na-accessible TiO_2–C microfibers (NTMFs-C) via emulsion ESP; the NTMFs-C delivered an enhanced capacity of 167 $mA{\cdot}h{\cdot}g^{-1}$ after 450 cycles at a current density of 50 $mA{\cdot}g^{-1}$, while retaining a capacity of 71 $mA{\cdot}h{\cdot}g^{-1}$ at the high current rate of 1 $A{\cdot}g^{-1}$ (Figs. 6(g)–(i)). Because of their thin TiO_2 inner walls and porous structure, the NTMFs-C exhibit fast Na^+ transport, high ion accessibility, and easy electron transport.

Recently, Gao et al. [12] fabricated Sn/SnO_2 at carbon nanofibers by means of ESP and an annealing method. These nanofibers

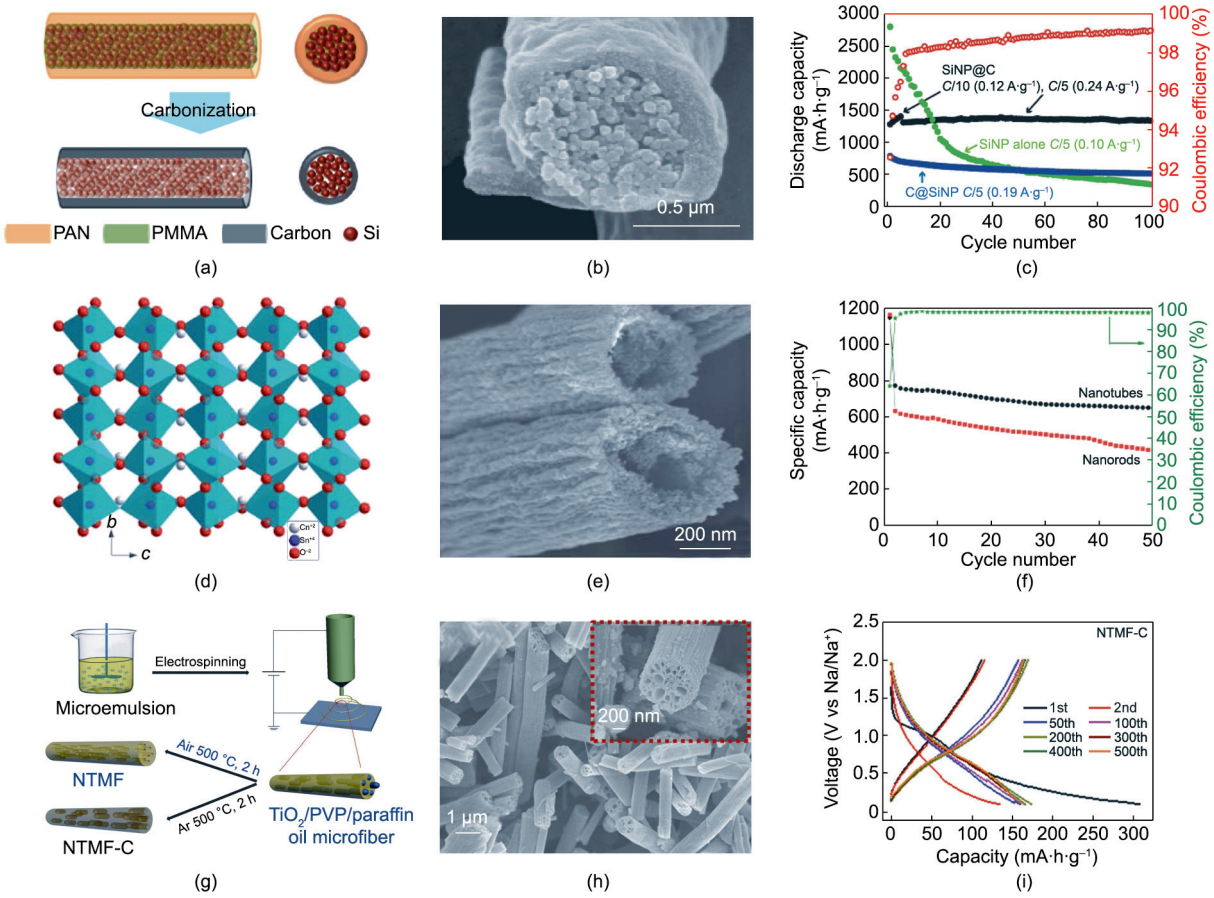

Fig. 6. (a) Schematic diagram of Si nanoparticles (SiNP) at C nanofiber carbonization steps (PMMA: poly(methyl methacrylate)). (b) SEM image of the SiNP at C core–shell nanofibers. (c) Cycling performance of SiNP at C core–shell nanofibers measured at a *C*/5 rate. (d) Crystal structure of $CaSnO_3$ nanotubes (CSO-NTs). (e) SEM image of CSO-NTs. (f) Cycling performance of CSO-NTs. (g) Schematic diagram of the synthetic processes for TiO_2 and TiO_2–C fibers via the ESP technique. (h) SEM images of TiO_2–C microfibers. (i) Charge/discharge curves of TiO_2–C fibers. (a–c) Reproduced from Ref. [76] with permission; (d–f) reproduced from Ref. [77] with permission; (g–i) reproduced from Ref. [56] with permission.

provided effective contact between the electrolyte and electrode materials due to their special structure, which possesses abundant inner spaces and a larger specific surface area. After 2000 cycles, the electrode materials exhibited a high specific capacity of 986 mA·h·g^{-1}. This excellent electrochemical performance indicates that Sn/SnO_2 at carbon hollow nanofibers have promising applications in high-performance LIBs.

3.1.2. Li–S batteries

Li–S batteries have attracted a great deal of attention because their theoretical specific energy is much higher than that of commercial LIBs [78–81]. Li–S batteries have thus become a powerful contender for future energy storage devices in electric vehicles and portable electronics [38]. However, the serious "shuttle effect" and the severe lithium dendrites are the main adverse factors hindering the development of Li–S batteries [24,82,83]. ESP nanofibers, due to their superior structures, exhibit unique properties that could solve the aforementioned problems.

Recently, researchers have explored the application of multi-structure nanofibers in Li–S batteries. Wu et al. [84] fabricated meso-hollow and microporous carbon nanofibers (MhMpCFs) via coaxial ESP followed by carbonization. As shown in Figs. 7(a) and (b) [84], the MhMpCFs were thermal treated with sulfur powder to form a S/MhMpCFs composite, which was used as the electrode material in Li–S batteries. The micropores effectively encapsulated the sulfur (S) active material and alleviated the dissolution of soluble polysulfides in the electrolyte, while the mesopores provided channels for rapid diffusion of lithium ions. Electrochemical studies showed that the maximum capacity of the S/MhMpCFs electrode material was 815 mA·h·g^{-1}, and its capacity was maintained at 715 mA·h·g^{-1} after 70 cycles (Fig. 7(c)), corresponding to a retention of 88%. This work and other earlier studies [85,86] have inspired the application of multi-structure materials prepared by ESP in the field of lithium batteries.

Li et al. [22] successfully fabricated three-dimensional (3D) networks of lotus-root-like multichannel carbon (LRC) nanofibers via ESP (Figs. 7(d) and (e)). Through a simple dip-and-dry method, the LRC loaded with S powder was tightly wrapped by an ethylenediamine-functionalized reduced graphene oxide (EFG) layer; the resulting material was termed LRC/S@EFG. The LRC/S@EFG effectively enhanced the cycling stability of the electrode. The capacity was also increased to more than 8 mA·h·cm^{-2} (Fig. 7(f)). Thus, these ESP nanofibers are having a positive impact on the development of high-performance batteries.

In addition to the aforementioned carbon fibers, transition-metal compound fibers can be prepared by ESP and fiber post-treatment technology for application in the energy field. Liao et al. [87] designed root-like TiN/C nanofibers for Li–S batteries as a freestanding host (Figs. 7(g) and (h)). These TiN/C nanofibers demonstrated excellent high-sulfur utilization and rate capability. For TiN/C materials with 4.0 mg·cm^{-2} S loading, a high stable capacity of 983 mA·h·g^{-1} was maintained at 0.2*C* (Fig. 7(i)). This performance improvement benefited from the multi-structure TiN/C nanofibers: ① The abundant vesicles in the root-like

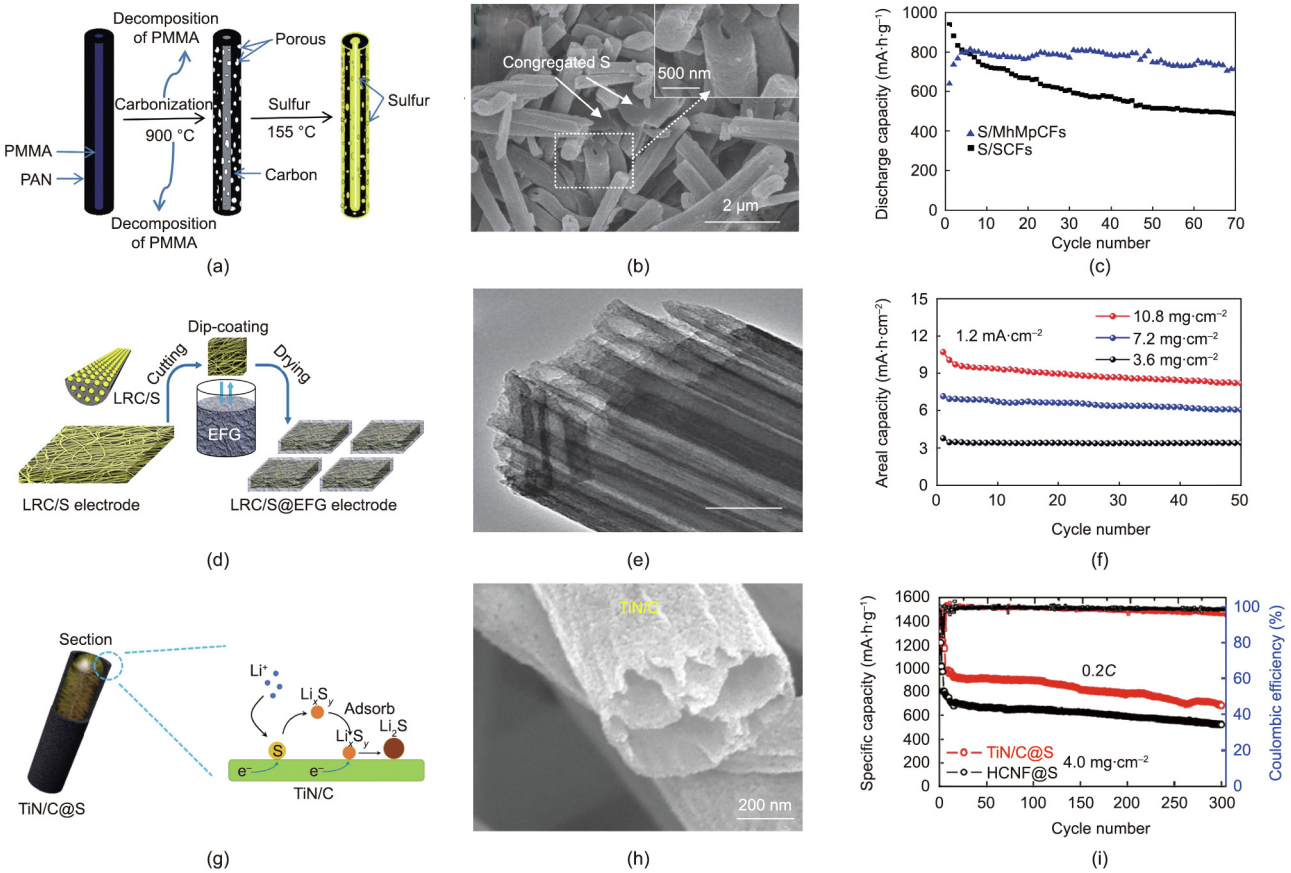

Fig. 7. (a) Schematic diagram of the synthesis processes of the S/MhMpCFs composite. (b) SEM image of the S/MhMpCFs composite. (c) Cycling performance of the S/MhMpCFs composite (SCF: solid carbon nanofiber). (d) Synthesis process of LRC nanofibers loaded with sulfur and coated ethylenediamine-functionalized reduced graphene oxide (EFG) (LRC/S@EFG). (e) TEM image of LRC (scale bar: 200 nm). (f) Areal capacities of LRC/S@EFG electrodes during cycling. (g) Schematic diagram of the electrode process for the TiN/C at S cathode. (h) SEM image of TiN/C nanofibers. (i) Cycle life and Coulombic efficiency of TiN/C at S electrodes with 4.0 mg·cm^{-2} S loading (HCNF: hollow carbon nanofiber). (a–c) Reproduced from Ref. [84] with permission; (d–f) reproduced from Ref. [22] with permission; (g–i) reproduced from Ref. [87] with permission.

nanofibers provided space to relieve the volume expansion; and ② the TiN anchored the polysulfides and boosted the electrochemistry reaction. The use of this unique structure is expected to result in high performance and high S-containing cathodes, which are favorable for the practical application of Li–S battery technology.

3.2. Nanofiber application in catalysis

Compared with routine bulk materials, ESP nanofibers possess greater specific areas, more active sites, and a more active lattice plane, which endow them with great potential in catalysis [25,88]. In particular, multi-structure nanofiber materials with hollow, core–shell, or multichannel structures have broad prospects in the field of catalysis [89].

Wang et al. [90] developed a novel methodology to fabricate TiO_2–SiO_2 nanofibers with a tunable porous structure by means of single-spinneret ESP (Fig. 8(a)). The mesoporous composite nanofibers of TiO_2–SiO_2 containing an appropriate ratio of anatase/rutile exhibited excellent photocatalytic activity in the degradation of rhodamine B (RhB). Under light, TS-8.08 (TS-*n*, where *n* is the Ti/Si molar ratio) degraded around 94% of the RhB in 20 min, and the degradation of RhB was complete in 50 min (Fig. 8(b)). The degradation rate constants of RhB by means of TS-8.08 and Degussa P25 were 0.1071 and 0.0895 per minute respectively, showing that TS-8.08 degrades RhB faster than Degussa P25 (Fig. 8(c)). The combination of high RhB adsorption and the high specific surface area of TS-8.08 allowed the RhB easy accessibility to the active sites, resulting in excellent photodegradation activity. This work opens up a new direction toward the advanced application of rationally designed hetero-structure inorganic fibers and tunable interconnected porous hierarchical structures.

Functionalized hollow structured fibers also have unique advantages in catalysis. Kang and Hwang [91] successfully fabricated hollow activated carbon nanofibers (HACNFs) embedded with Mn_3O_4 nanoparticles (Mn_3O_4/HACNFs) (Fig. 8(d)). Because of the hollow structure, the adsorption capacity of the Mn_3O_4/HACNFs to toluene was very strong. Compared with traditional activated carbon nanofibers, the adsorption breakthrough time of toluene was longer, as shown in Figs. 8(e) and (f). These results indicate that Mn_3O_4/HACNFs have potential for capturing volatile organic compounds.

Materials with a hierarchical porous structure have been applied in some fields because of their ready mass transfer properties [92,93]. In fibrous materials, due to the large ratio of length to diameter, the inner surfaces of hollow fibers cannot be used effectively. Yue et al. [94] developed hollow through-hole TiO_2 nanofibers with gold (Au) nanoparticles (Au/TiO_2 HTHNFs) via a coaxial ESP method (Fig. 8(g)). The Au/TiO_2 HTHNFs exhibited high catalytic activity (Fig. 8(h)) and cyclical stability (Fig. 8(i)) in a liquid-phase 4-nitrophenol reduction reaction. The through-holes on the nanofibers provided enough mass transfer channels for the reactants to enter the inner space, which permitted the exchange of reactants and products between the inner space and the outside space. The active molecules were quickly refreshed,

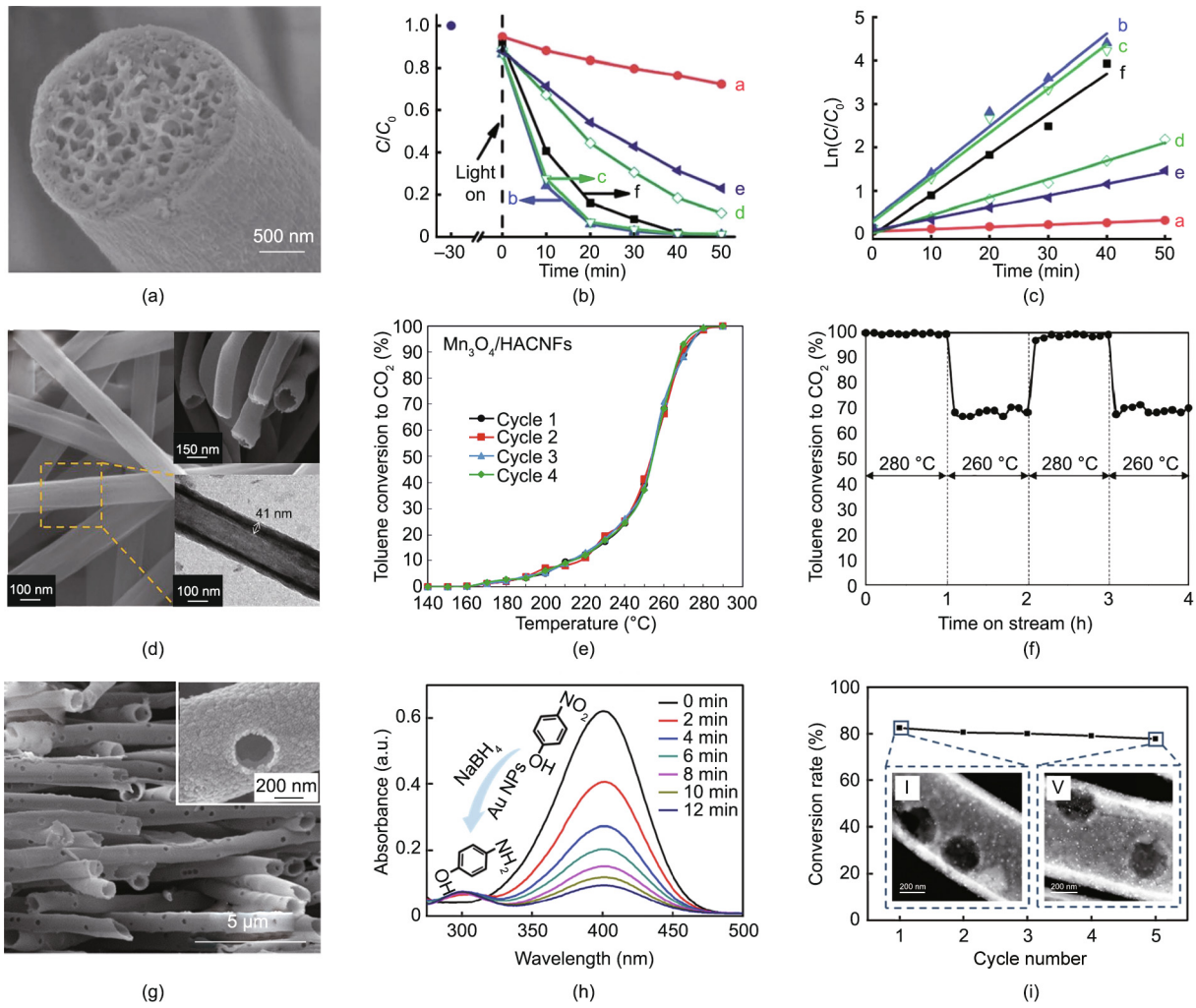

Fig. 8. (a–c) TiO_2–SiO_2 composite nanofibers for photocatalysis: (a) SEM image of porous TiO_2–SiO_2 composite nanofibers; (b) photocatalytic degradation of rhodamine B (RhB) monitored at normalized concentration change (C/C_0) vs irradiation time (t) (a: TS-N; b: TS-8.08; c: TS-5.41; d: TS-2.53; e: TS-1.18; f: P25); (c) reaction rate constants associated with RhB photodegradation (a: TS-N; b: TS-8.08; c: TS-5.41; d: TS-2.53; e: TS-1.18; f: P25). (d–f) Mn_3O_4 nanoparticles embedded in hollow activated carbon nanofibers (Mn_3O_4/HACNFs) for toluene removal: (d) SEM and TEM images of hollow nanofibers; (e) reusability tests of Mn_3O_4/HACNFs for the total oxidation of toluene; (f) evolution of conversion to CO_2 with the time on stream of Mn_3O_4/HACNFs. (g–i) Au/TiO_2 hollow through-hole nanofibers (Au/TiO_2 HTHNFs) for photocatalysis: (g) SEM images of TiO_2 HTHNFs; (h) ultraviolet/visible (UV/vis) absorption spectrum of the reaction solution with different reaction times (a.u.: arbitrary unit); (i) catalytic activity of Au/TiO_2 HTHNFs in reduction showing a negligible decrease in five cycles. (a–c) Reproduced from Ref. [90] with permission; (d–f) reproduced from Ref. [91] with permission; (g–i) reproduced from Ref. [94] with permission.

which increased the reaction rate. Therefore, the reaction rate was significantly increased by mass transfer enhancement. This strategy of mass transfer enhancement can easily be extended to many hollow nanomaterials, with promising applications in the catalyst and energy fields.

3.3. Nanofiber application in biology

ESP fiber systems are widely used in various fields due to their diverse structure and adjustable porosity [2,95–98]. The excellent intrinsic properties of nanofibers, which include structural diversity and high porosity, are beneficial for the loading and release of various drugs [58]. ESP nanofibers can mimic the extracellular matrix (ECM) and are used in tissue engineering as promising two-dimensional (2D) or 3D scaffolds.

3.3.1. Drug delivery

Because of their diverse structures, ESP nanofibers have adjustable surface properties; they can also be similar to the ECM [99]. These properties give nanofibers the following advantages in drug delivery: ① The diversity of polymer species can be adapted to many reagents with different physicochemical properties [100]; and ② the unique physicochemical properties of polymers enable high drug loading and high encapsulation efficiency [58]. These advantages of ESP fibers have laid a solid foundation for their future development, making it possible to develop commercial products based on ESP.

Due to their ability to carry drugs, nanocarriers have attracted wide attention in cancer therapy, although their applications are still limited due to their low delivery efficiency of intravenous chemotherapy drugs. Yang et al. [101] developed a local drug-delivery device combining implantable polymeric nanofibers and an active targeting micellar system (Fig. 9(a)). This design was achieved by hydrophobic doxorubicin (DOX)-encapsulated active targeted micelles. The core/shell nanofibers, which had poly(vinyl alcohol) (PVA) and the micelles as the core region and gelatin as the outer region, were prepared by coaxial ESP, as shown in Fig. 9(b). The implantable device, when equipped with agents of low-dose therapy, can ensure long-term drug concentrations at tumor sites while maintaining low systemic drug exposure to

normal tissues, compared with the usual delivery strategies for repeated intravenous micelle therapy. Moreover, these micelles can be further internalized into tumor cells through receptor-mediated endocytosis, thus producing higher therapeutic effects on tumor cells and lower toxicity to normal tissues (Fig. 9(c)). In addition, this implantable device can greatly reduce the frequency of dosing and has the potential to improve the life quality and compliance of patients. The study opens up new possibilities for developing implantable devices for safe cancer treatment.

Due to the quick degradation of mycophenolic acid (MPA), the development of an anti-tumor therapy based on MPA has been hampered. To resolve this problem, Han et al. [102] prepared MPA-containing ESP coaxial fibers as a local drug-delivery vehicle (Fig. 9(d)). These fibers, which had poly(ε-caprolactone) (PCL)-MPA or PVP-MPA as the core region and PCL as the outer layer, provided an excellent slow released effect in comparison with common fibers (Fig. 9(e)). A thicker PCL shell provided gradual release in the initial period and higher MPA release after the media had been refreshed. The structure of the fibers had a significant effect on the release of MPA, with coaxial fibers with a PVP-MPA core and PCL sheath exhibiting better sustained release than PCL-MPA and PVP-MPA fibers, as shown in Figs. 9(f) and (g). This study indicates that MPA-containing ESP fibers have great potential for the local treatment of glioblastoma multiforme.

3.3.2. Tissue engineering

In recent years, ESP fibers have been widely used in tissue engineering due to their similar structure to the natural fiber structures of the ECM [105]. Xu et al. [103] prepared a bicomponent scaffold with island-like core–shell fibers that combined the respective advantages of chitosan (CS) and polylactic acid (PLA) via ESP (Figs. 10(a) and (b)). The results of implanting preosteoblast (MC3T3-E1) cells on the modified scaffold showed that the CS components and rough surface structure balanced the hydrophilicity and hydrophobicity of the fiber and provided convenient conditions for cell attachment and growth. The "island-like" structure and CS on the coaxial nanofiber surface increased the cell activity and provided more appropriate conditions for cell proliferation (Figs. 10(b) and (c)). This research provides a new way for the design of PLA scaffolds, which can be applied in biomedicine to the surface between materials and cells, combining topography and bioactive modification effects.

The presence of osteoconductive and osteoinductive factors plays an important role in promoting the differentiation of stem cells into osteogenic lines. Shalumon et al. [104] prepared silk fibroin (SF)/CS/nanohydroxyapatite (nHAP)/bone morphogenetic protein-2 (BMP-2) (SCHB2) nanofiber membrane (NFM) with BMP-2 as the core and SF/CS/nHAP as the shell of nanofibers (Figs. 10(e) and (f)). The BMP-2 released from the nanofibers exhibited bone-induced activity in human-bone-marrow-derived mesenchymal stem cells (hMSCs). The incorporation of the BMP-2 promoted the osteogenic differentiation of hMSCs; thus, the SCHB2-thin NFMs, in comparison with SF/CS and SF/CS/nHAP NFMs, were shown to be the best scaffold material for cell culture *in vitro* (Fig. 10(g)) [104]. Hence, SCHB2-thin NFMs may be considered as a potential material for bone-specific tissue regeneration.

4. Summary

In summary, multi-fluidic ESP technology is a very simple and general method for preparing multi-structure nanofibers with different functions. Given the advantages of fiber materials and the demand for novel functional materials, multi-structure nanofibers show great potential in many areas, including energy (LIBs, SIBs, and Li–S batteries), catalysis, and biology (drug delivery and tissue engineering), which were highlighted in this review.

5. Challenges and outlook

ESP technology has become an important method for preparing nanofibers. However, some problems remain to be addressed prior to widespread nanofiber application.

(1) **Mass production.** Low productivity is the main disadvantage in the commercial application of ESP nanofiber materials—

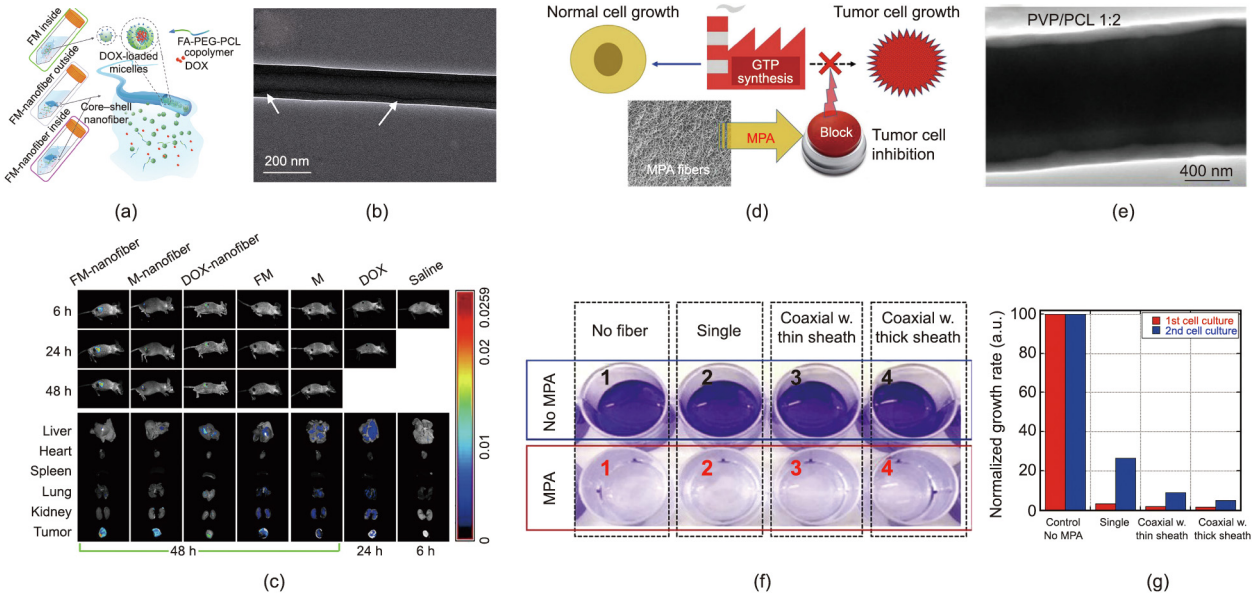

Fig. 9. (a–c) Core/shell poly(ethylene glycol) (PEG)/poly(ε-caprolactone) (PCL) nanofibers for drug release: (a) schematic diagram of the drug release (FA: folic acid; DOX: doxorubicin; FM: DOX-loaded FA-decorated micelle); (b) TEM image of micelle-encapsulated PEG/PCL nanofiber; (c) *in vivo* and *ex vivo* DOX fluorescence images (M: micelle). The fibers of the core–shell structure ensure that there are therapeutic drug levels at the tumor site. (d–g) Core/shell (PVP-MPA)/PCL nanofibers for drug release: (d) schematic diagram of the effect of MPA on brain tumor cells (GTP: guanosine-5′-triphosphate); (e) TEM observation of PVP/PCL coaxial fiber; (f) photos of glioblastoma multiforme cell cultures exposed to MPA-containing fiber membranes and control samples after one week (w.: with); (g) relative growth rate of tumor cell cultures exposed to different materials. (a–c) Reproduced from Ref. [101] with permission; (d–g) reproduced from Ref. [102] with permission.

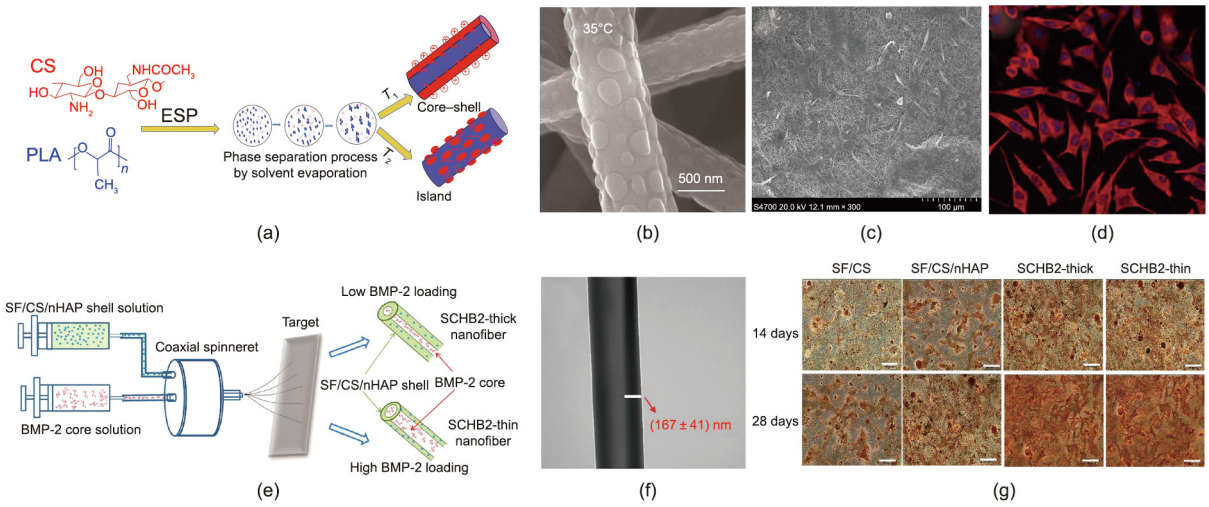

Fig. 10. (a) The preparation process of chitosan (CS) islanded structured scaffolds. (b) SEM images of ESP polylactic acid (PLA)/CS nanofibers. (c) SEM and (d) laser confocal scanning microscope micrographs of cells grown and attached for 48 h. (e) Schematic diagram of the preparation of silk fibroin (SF)/CS/nanohydroxyapatite (nHAP)/bone morphogenetic protein-2 (BMP-2) (SCHB2) nanofibrous membranes (NFMs) through coaxial ESP. (f) TEM image of SCHB2-thick. (g) Von Kossa staining of the mineral deposition of human bone-marrow-derived mesenchymal stem cells (hMSCs) cultured on different NFMs for 14 and 28 days (scale bar: 200 μm). (a–d) Reproduced from Ref. [103] with permission; (e–g) reproduced from Ref. [104] with permission.

especially multi-structure nanofiber materials. Thus far, many pieces of ESP equipment have been developed for the large-scale production of nanofibers. Although these approaches can fabricate simple solid nanofiber materials, they are still unsuitable for the preparation of multifunctional, multi-structure nanofiber materials.

(2) **Multi-structural controllability.** Many factors, such as temperature, humidity, the feed rate of soluble polymers, and so on, affect the preparation of ESP materials. In particular, when more complex multi-fluidic ESP is involved, the spinnability of multiple polymers and the yield of multi-structure fibers are greatly impacted. Therefore, one direction for future efforts should be to optimize the spinning conditions and design more reliable equipment.

(3) **Practicability of multi-structure nanofibers.** Although multi-structure nanofibers have been used in many fields, their irreplaceable applications remain vague.

(4) **Lack of clarity on mechanisms.** For a multi-fluid and complex ESP system, the specific response process of the multi-polymer solution and the electric field remains unclear.

Although many technical problems and parameters remain to be improved, there is no doubt that multi-fluidic ESP has the potential to be one of the most powerful technologies for the preparation of materials with multifunctional properties. ESP materials will also play an increasingly important role in production, providing exciting opportunities for development in the fields of energy, the environment, catalysis, biology, photonics, and electronics. Optimizing the structure and composition of nanofibers will open up new fields for the preparation of various functional materials in the future.

Acknowledgments

The authors acknowledge the National Natural Science Foundation of China (22175007, 21975007, 21774005, and 21433012), the National Natural Science Foundation for Outstanding Youth Foundation, the Fundamental Research Funds for the Central Universities, the National Program for Support of Top-Notch Young Professionals, the 111 project (B14009), the National Postdoctoral Program for Innovative Talents (BX20190027), and the China Postdoctoral Science Foundation Funded Project (2019M650431).

Compliance with ethics guidelines

Dianming Li, Guichu Yue, Shuai Li, Jing Liu, Huaike Li, Yuan Gao, Jingchong Liu, Lanlan Hou, Xiaofeng Liu, Zhimin Cui, Nü Wang, Jie Bai, and Yong Zhao declare that they have no conflict of interest or financial conflicts to disclose.

References

[1] Peng S, Jin G, Li L, Li K, Srinivasan M, Ramakrishna S, et al. Multi-functional electrospun nanofibres for advances in tissue regeneration, energy conversion & storage, and water treatment. Chem Soc Rev 2016;45(5):1225–41.
[2] Sridhar R, Lakshminarayanan R, Madhaiyan K, Amutha Barathi V, Lim KH, Ramakrishna S. Electrosprayed nanoparticles and electrospun nanofibers based on natural materials: applications in tissue regeneration, drug delivery and pharmaceuticals. Chem Soc Rev 2015;44(3):790–814.
[3] Jin T, Han Q, Wang Y, Jiao L. 1D nanomaterials: design, synthesis, and applications in sodium-ion batteries. Small 2018;14(2):1703086.
[4] Cavaliere S, Subianto S, Savych I, Jones DJ, Rozière J. Electrospinning: designed architectures for energy conversion and storage devices. Energy Environ Sci 2011;4(12):4761–85.
[5] Tan X, Rodrigue D. A review on porous polymeric membrane preparation. Part I: production techniques with polysulfone and poly (vinylidene fluoride). Polymers 2019;11(7):1160.
[6] Quirós J, Boltes K, Rosal R. Bioactive applications for electrospun fibers. Polym Rev 2016;56(4):631–67.
[7] Liu J, Zhang F, Hou L, Li S, Gao Y, Xin Z, et al. Synergistic engineering of 1D electrospun nanofibers and 2D nanosheets for sustainable applications. Sustain Mater Technol 2020;26:e00214.
[8] Jiang S, Chen Y, Duan G, Mei C, Greiner A, Agarwal S. Electrospun nanofiber reinforced composites: a review. Polym Chem 2018;9(20):2685–720.
[9] Yue G, Wang Y, Li D, Hou L, Cui Z, Li Q, et al. Bioinspired surface with special wettability for liquid transportation and separation. Sustain Mater Technol 2020;25:e00175.
[10] Zhang CL, Yu SH. Nanoparticles meet electrospinning: recent advances and future prospects. Chem Soc Rev 2014;43(13):4423–48.
[11] Wu J, Wang N, Wang L, Dong H, Zhao Y, Jiang L. Unidirectional water-penetration composite fibrous film via electrospinning. Soft Matter 2012;8(22):5996–9.
[12] Gao S, Wang N, Li S, Li D, Cui Z, Yue G, et al. A multi-wall Sn/SnO_2@carbon hollow nanofiber anode material for high-rate and long-life lithium-ion batteries. Angew Chem Int Ed Engl 2020;59(6):2465–72.
[13] Liu K, Wang N, Wang W, Shi L, Li H, Guo F, et al. A bio-inspired high strength three-layer nanofiber vascular graft with structure guided cell growth. J Mater Chem B 2017;5(20):3758–64.
[14] Loscertales IG, Barrero A, Guerrero I, Cortijo R, Marquez M, Gañán-Calvo AM. Micro/nano encapsulation via electrified coaxial liquid jets. Science 2002;295(5560):1695–8.
[15] Li L, Peng S, Lee JKY, Ji D, Srinivasan M, Ramakrishna S. Electrospun hollow nanofibers for advanced secondary batteries. Nano Energy 2017;39:111–39.

[16] Liu J, Jiang G, Liu Y, Di J, Wang Y, Zhao Z, et al. Hierarchical macro–meso–microporous ZSM-5 zeolite hollow fibers with highly efficient catalytic cracking capability. Sci Rep 2015;4(1):7276.
[17] Wu Y, Hu S, Xu R, Wang J, Peng Z, Zhang Q, et al. Boosting potassium-ion battery performance by encapsulating red phosphorus in free-standing nitrogen-doped porous hollow carbon nanofibers. Nano Lett 2019;19(2):1351–8.
[18] Birajdar MS, Lee J. Sonication-triggered zero-order release by uncorking core–shell nanofibers. Chem Eng J 2016;288:1–8.
[19] Chen H, Zhao Y, Song Y, Jiang L. One-step multicomponent encapsulation by compound-fluidic electrospray. J Am Chem Soc 2008;130(25):7800–1.
[20] Cai M, He H, Zhang X, Yan Xu, Li J, Chen F, et al. Efficient synthesis of PVDF/PI side-by-side bicomponent nanofiber membrane with enhanced mechanical strength and good thermal stability. Nanomaterials 2018;9(1):39.
[21] Lin T, Wang H, Wang X. Self-crimping bicomponent nanofibers electrospun from polyacrylonitrile and elastomeric polyurethane. Adv Mater 2005;17(22):2699–703.
[22] Li Z, Zhang JT, Chen YM, Li J, Lou XW. Pie-like electrode design for high-energy density lithium–sulfur batteries. Nat Commun 2015;6(1):8850.
[23] Nikmaram N, Roohinejad S, Hashemi S, Koubaa M, Barba FJ, Abbaspourrad A, et al. Emulsion-based systems for fabrication of electrospun nanofibers: food, pharmaceutical and biomedical applications. RSC Adv 2017;7(46):28951–64.
[24] Yang Y, Wang S, Zhang L, Deng Y, Xu H, Qin X, et al. CoS-interposed and Ketjen black-embedded carbon nanofiber framework as a separator modulation for high performance Li–S batteries. Chem Eng J 2019;369:77–86.
[25] Li S, Cui Z, Li D, Yue G, Liu J, Ding H, et al. Hierarchically structured electrospinning nanofibers for catalysis and energy storage. Compos Commun 2019;13:1–11.
[26] Gao X, Han S, Zhang R, Liu G, Wu J. Progress in electrospun composite nanofibers: composition, performance and applications for tissue engineering. J Mater Chem B 2019;7(45):7075–89.
[27] Wang W, Zhang MJ, Chu LY. Functional polymeric microparticles engineered from controllable microfluidic emulsions. Acc Chem Res 2014;47(2):373–84.
[28] Deng NN, Sun J, Wang W, Ju XJ, Xie R, Chu LY. Wetting-induced coalescence of nanoliter drops as microreactors in microfluidics. ACS Appl Mater Interfaces 2014;6(6):3817–21.
[29] Wu B, Yang C, Li B, Feng L, Hai M, Zhao CX, et al. Active encapsulation in biocompatible nanocapsules. Small 2020;16(30):2002716.
[30] Yuan Y, Brouchon J, Calvo-Calle JM, Xia J, Sun L, Zhang X, et al. Droplet encapsulation improves accuracy of immune cell cytokine capture assays. Lab Chip 2020;20(8):1513–20.
[31] Shah RK, Shum HC, Rowat AC, Lee D, Agresti JJ, Utada AS, et al. Designer emulsions using microfluidics. Mater Today 2008;11(4):18–27.
[32] He H, Yang C, Wang F, Wei Z, Shen J, Chen D, et al. Mechanically strong globular-protein-based fibers obtained using a microfluidic spinning technique. Angew Chem Int Ed Engl 2020;59(11):4344–8.
[33] Deng Ke, Liu Z, Luo F, Xie R, He XH, Jiang MY, et al. Controllable fabrication of polyethersulfone hollow fiber membranes with a facile double co-axial microfluidic device. J Membr Sci 2017;526:9–17.
[34] Utada AS, Lorenceau E, Link DR, Kaplan PD, Stone HA, Weitz DA. Monodisperse double emulsions generated from a microcapillary device. Science 2005;308(5721):537–41.
[35] Ahn K, Agresti J, Chong H, Marquez M, Weitz DA. Electrocoalescence of drops synchronized by size-dependent flow in microfluidic channels. Appl Phys Lett 2006;88(26):264105.
[36] Xue J, Wu T, Dai Y, Xia Y. Electrospinning and electrospun nanofibers: methods, materials, and applications. Chem Rev 2019;119(8):5298–415.
[37] Lu X, Wang C, Favier F, Pinna N. Electrospun nanomaterials for supercapacitor electrodes: designed architectures and electrochemical performance. Adv Energy Mater 2017;7(2):1601301.
[38] Liu M, Deng N, Ju J, Fan L, Wang L, Li Z, et al. Electrospun nanofiber materials for lithium–sulfur batteries. Adv Funct Mater 2019;29(49):1905467.
[39] Robinson TM, Hutmacher DW, Dalton PD. The next frontier in melt electrospinning: taming the jet. Adv Funct Mater 2019;29(44):1904664.
[40] Xue J, Xie J, Liu W, Xia Y. Electrospun nanofibers: new concepts, materials, and applications. Acc Chem Res 2017;50(8):1976–87.
[41] Hou L, Wang N, Man X, Cui Z, Wu J, Liu J, et al. Interpenetrating Janus membrane for high rectification ratio liquid unidirectional penetration. ACS Nano 2019;13(4):4124–32.
[42] Hou LL, Wang N, Wu J, Cui ZM, Jiang L, Zhao Y. Bioinspired superwettability electrospun micro/nanofibers and their applications. Adv Funct Mater 2018;28(49):1801114.
[43] Han D, Steckl AJ. Coaxial electrospinning formation of complex polymer fibers and their applications. ChemPlusChem 2019;84(10):1453–97.
[44] Li D, Xia Y. Direct fabrication of composite and ceramic hollow nanofibers by electrospinning. Nano Lett 2004;4(5):933–8.
[45] McClellan P, Landis WJ. Recent applications of coaxial and emulsion electrospinning methods in the field of tissue engineering. Biores Open Access 2016;5(1):212–7.
[46] Lu Y, Huang J, Yu G, Cardenas R, Wei S, Wujcik EK, et al. Coaxial electrospun fibers: applications in drug delivery and tissue engineering. Wires Nanomed Nanobiotechno 2016;8(5):654–77.
[47] Li F, Zhao Y, Wang S, Han D, Jiang L, Song Y. Thermochromic core–shell nanofibers fabricated by melt coaxial electrospinning. J Appl Polym Sci 2009;112(1):269–74.
[48] Chen H, Wang N, Di J, Zhao Y, Song Y, Jiang L. Nanowire-in-microtube structured core/shell fibers via multifluidic coaxial electrospinning. Langmuir 2010;26(13):11291–6.
[49] Yoon KR, Lee GY, Jung JW, Kim NH, Kim SO, Kim ID. One-dimensional RuO_2/Mn_2O_3 hollow architectures as efficient bifunctional catalysts for lithium–oxygen batteries. Nano Lett 2016;16(3):2076–83.
[50] Walia N, Dasgupta N, Ranjan S, Ramalingam C, Gandhi M. Methods for nanoemulsion and nanoencapsulation of food bioactives. Environ Chem Lett 2019;17(4):1471–83.
[51] Zhao Y, Cao X, Jiang L. Bio-mimic multichannel microtubes by a facile method. J Am Chem Soc 2007;129(4):764–5.
[52] Ma Q, Wang J, Dong X, Yu W, Liu G. Flexible Janus nanoribbons array: a new strategy to achieve excellent electrically conductive anisotropy, magnetism, and photoluminescence. Adv Funct Mater 2015;25(16):2436–43.
[53] Zhao L, Xie S, Liu Y, Liu Q, Song X, Li X. Janus micromotors for motion-capture-lighting of bacteria. Nanoscale 2019;11(38):17831–40.
[54] Roh KH, Martin DC, Lahann J. Biphasic Janus particles with nanoscale anisotropy. Nat Mater 2005;4(10):759–63.
[55] Jalani G, Jung CW, Lee JS, Lim DW. Fabrication and characterization of anisotropic nanofiber scaffolds for advanced drug delivery systems. Int J Nanomed 2014;9(Suppl 1):33–49.
[56] Wang N, Gao Y, Wang YX, Liu K, Lai W, Hu Y, et al. Nanoengineering to achieve high sodium storage: a case study of carbon coated hierarchical nanoporous TiO_2 microfibers. Adv Sci 2016;3(8):1600013.
[57] Li X, Sun Y, Xu X, Wang YX, Chou SL, Cao A, et al. Lotus rhizome-like S/N–C with embedded WS_2 for superior sodium storage. J Mater Chem A 2019;7(45):25932–43.
[58] Yang G, Li X, He Y, Ma J, Ni G, Zhou S. From nano to micro to macro: electrospun hierarchically structured polymeric fibers for biomedical applications. Prog Polym Sci 2018;81:80–113.
[59] Shang L, Yu Y, Liu Y, Chen Z, Kong T, Zhao Y. Spinning and applications of bioinspired fiber systems. ACS Nano 2019;13(3):2749–72.
[60] Wang X, Ding B, Yu J, Wang M. Engineering biomimetic superhydrophobic surfaces of electrospun nanomaterials. Nano Today 2011;6(5):510–30.
[61] Wang Y, Chen C, Xie H, Gao T, Yao Y, Pastel G, et al. 3D-printed all-fiber Li-ion battery toward wearable energy storage. Adv Funct Mater 2017;27(43):1703140.
[62] Wang T, Kim HK, Liu Y, Li W, Griffiths JT, Wu Y, et al. Bottom-up formation of carbon-based structures with multilevel hierarchy from MOF-guest polyhedra. J Am Chem Soc 2018;140(19):6130–6.
[63] Ladpli P, Nardari R, Kopsaftopoulos F, Chang FK. Multifunctional energy storage composite structures with embedded lithium-ion batteries. J Power Sources 2019;414:517–29.
[64] Rao J, Liu N, Zhang Z, Su J, Li L, Xiong L, et al. All-fiber-based quasi-solid-state lithium-ion battery towards wearable electronic devices with outstanding flexibility and self-healing ability. Nano Energy 2018;51:425–33.
[65] Weng W, Sun Q, Zhang Ye, Lin H, Ren J, Lu X, et al. Winding aligned carbon nanotube composite yarns into coaxial fiber full batteries with high performances. Nano Lett 2014;14(6):3432–8.
[66] Cui J, Zhan TG, Zhang KD, Chen D. The recent advances in constructing designed electrode in lithium metal batteries. Chin Chem Lett 2017;28(12):2171–9.
[67] Zhang XQ, Zhao CZ, Huang JQ, Zhang Q. Recent advances in energy chemical engineering of next-generation lithium batteries. Engineering 2018;4(6):831–47.
[68] Dong S, Li C, Ge X, Li Z, Miao X, Yin L. ZnS–Sb_2S_3@C core–double shell polyhedron structure derived from metal–organic framework as anodes for high performance sodium ion batteries. ACS Nano 2017;11(6):6474–82.
[69] Sun J, Lv C, Lv F, Chen S, Li D, Guo Z, et al. Tuning the shell number of multishelled metal oxide hollow fibers for optimized lithium-ion storage. ACS Nano 2017;11(6):6186–93.
[70] Wu J, Qin X, Miao C, He YB, Liang G, Zhou D, et al. A honeycomb-cobweb inspired hierarchical core–shell structure design for electrospun silicon/carbon fibers as lithium-ion battery anodes. Carbon 2016;98:582–91.
[71] Zhang H, Qin X, Wu J, He YB, Du H, Li B, et al. Electrospun core–shell silicon/carbon fibers with an internal honeycomb-like conductive carbon framework as an anode for lithium ion batteries. J Mater Chem A 2015;3(13):7112–20.
[72] Zhou D, Song WL, Fan LZ. Hollow core–shell SnO_2/C fibers as highly stable anodes for lithium-ion batteries. ACS Appl Mater Interfaces 2015;7(38):21472–8.
[73] Zhu J, Wu Y, Huang X, Huang L, Cao M, Song G, et al. Self-healing liquid metal nanoparticles encapsulated in hollow carbon fibers as a free-standing anode for lithium-ion batteries. Nano Energy 2019;62:883–9.
[74] He Y, Zhang Y, Ding F, Li X, Wang Z, Lü Z, et al. Formation of hollow nanofiber rolls through controllable carbon diffusion for Li metal host. Carbon 2020;157:622–30.
[75] Chen YM, Yu L, Lou XW. Hierarchical tubular structures composed of Co_3O_4 hollow nanoparticles and carbon nanotubes for lithium storage. Angew Chem Int Ed Engl 2016;55(20):5990–3.
[76] Hwang TH, Lee YM, Kong BS, Seo JS, Choi JW. Electrospun core–shell fibers for robust silicon nanoparticle-based lithium ion battery anodes. Nano Lett 2012;12(2):802–7.
[77] Li L, Peng S, Cheah YL, Wang J, Teh P, Ko Y, et al. Electrospun eggroll-like $CaSnO_3$ nanotubes with high lithium storage performance. Nanoscale 2013;5(1):134–8.

[78] Wei H, Rodriguez EF, Best AS, Hollenkamp AF, Chen D, Caruso RA. Ordered mesoporous graphitic carbon/iron carbide composites with high porosity as a sulfur host for Li–S batteries. ACS Appl Mater Interfaces 2019;11(14):13194–204.
[79] Zeng Z, Li W, Wang Q, Liu X. Programmed design of a lithium–sulfur battery cathode by integrating functional units. Adv Sci 2019;6(17):1900711.
[80] Zhao M, Peng HJ, Zhang ZW, Li BQ, Chen X, Xie J, et al. Activating inert metallic compounds for high-rate lithium–sulfur batteries through *in situ* etching of extrinsic metal. Angew Chem Int Ed Engl 2019;58(12):3779–83.
[81] Shao Y, Wang Q, Hu L, Pan H, Shi X. BC_2N monolayers as promising anchoring materials for lithium–sulfur batteries: first-principles insights. Carbon 2019;149:530–7.
[82] Song C, Peng C, Bian Z, Dong F, Xu H, Yang J, et al. Stable and fast lithium–sulfur battery achieved by rational design of multifunctional separator. Energy Environ Mater 2019;2(3):216–24.
[83] Thangavel V, Guerrero OX, Quiroga M, Mikala AM, Rucci A, Franco AA. A three dimensional kinetic Monte Carlo model for simulating the carbon/sulfur mesostructural evolutions of discharging lithium sulfur batteries. Energy Storage Mater 2020;24:472–85.
[84] Wu Y, Gao M, Li X, Liu Y, Pan H. Preparation of mesohollow and microporous carbon nanofiber and its application in cathode material for lithium–sulfur batteries. J Alloys Compd 2014;608:220–8.
[85] Yao Yu, Wang H, Yang H, Zeng S, Xu R, Liu F, et al. A dual-functional conductive framework embedded with TiN–VN heterostructures for highly efficient polysulfide and lithium regulation toward stable Li–S full batteries. Adv Mater 2020;32(6):1905658.
[86] Li Lu, Hou L, Cheng J, Simmons T, Zhang F, Zhang LT, et al. A flexible carbon/sulfur-cellulose core–shell structure for advanced lithium–sulfur batteries. Energy Storage Mater 2018;15:388–95.
[87] Liao Y, Xiang J, Yuan L, Hao Z, Gu J, Chen X, et al. Biomimetic root-like TiN/C@S nanofiber as a freestanding cathode with high sulfur loading for lithium–sulfur batteries. ACS Appl Mater Interfaces 2018;10(44):37955–62.
[88] Cao X, Deng J, Pan K. Electrospinning Janus type CoO_x/C nanofibers as electrocatalysts for oxygen reduction reaction. Adv Fiber Mater 2020;2(2):85–92.
[89] Anis SF, Khalil A, Saepurahman, Singaravel G, Hashaikeh R. A review on the fabrication of zeolite and mesoporous inorganic nanofibers formation for catalytic applications. Microporous Mesoporous Mater 2016;236:176–92.
[90] Wang Y, Huang H, Gao J, Lu G, Zhao Y, Xu Y, et al. TiO_2–SiO_2 composite fibers with tunable interconnected porous hierarchy fabricated by single-spinneret electrospinning toward enhanced photocatalytic activity. J Mater Chem A 2014;2(31):12442.
[91] Kang S, Hwang J. Fabrication of hollow activated carbon nanofibers (HACNFs) containing manganese oxide catalyst for toluene removal via two-step process of electrospinning and thermal treatment. Chem Eng J 2020;379:122315.
[92] Jiang S, Lv LP, Landfester K, Crespy D. Nanocontainers in and onto nanofibers. Acc Chem Res 2016;49(5):816–23.
[93] Huang Y, Song J, Yang C, Long Y, Wu H. Scalable manufacturing and applications of nanofibers. Mater Today 2019;28:98–113.
[94] Yue G, Li S, Li D, Liu J, Wang Y, Zhao Y, et al. Coral-like Au/TiO_2 hollow nanofibers with through-holes as a high-efficient catalyst through mass transfer enhancement. Langmuir 2019;35(14):4843–8.
[95] Yang X, Li L, Yang D, Nie J, Ma G. Electrospun core–shell fibrous 2D scaffold with biocompatible poly(glycerol sebacate) and poly-*L*-lactic acid for wound healing. Adv Fiber Mater 2020;2(2):105–17.
[96] Guangming G, Juntao W, Yong Z, Jingang L, Xu J, Lei J. A novel fluorinated polyimide surface with petal effect produced by electrospinning. Soft Matter 2014;10(4):549–52.
[97] Huang C, Thomas NL. Fabrication of porous fibers via electrospinning: strategies and applications. Polym Rev 2019;60(4):595–647.
[98] Dong Y, Zheng Y, Zhang K, Yao Y, Wang L, Li X, et al. Electrospun nanofibrous materials for wound healing. Adv Fiber Mater 2020;2(4):212–27.
[99] Abdullah MF, Nuge T, Andriyana A, Ang BC, Muhamad F. Core–shell fibers: design, roles, and controllable release strategies in tissue engineering and drug delivery. Polymers 2019;11(12):2008.
[100] Karger-Kocsis J, Kéki S. Review of progress in shape memory epoxies and their composites. Polymers 2017;10(1):34.
[101] Yang G, Wang J, Wang Y, Li L, Guo X, Zhou S. An implantable active-targeting micelle-in-nanofiber device for efficient and safe cancer therapy. ACS Nano 2015;9(2):1161–74.
[102] Han D, Sasaki M, Yoshino H, Kofuji S, Sasaki AT, Steckl AJ. *In-vitro* evaluation of MPA-loaded electrospun coaxial fiber membranes for local treatment of glioblastoma tumor cells. J Drug Deliv Sci Technol 2017;40:45–50.
[103] Xu T, Yang H, Yang D, Yu ZZ. Polylactic acid nanofiber scaffold decorated with chitosan island-like topography for bone tissue engineering. ACS Appl Mater Interfaces 2017;9(25):21094–104.
[104] Shalumon KT, Lai GJ, Chen CH, Chen JP. Modulation of bone-specific tissue regeneration by incorporating bone morphogenetic protein and controlling the shell thickness of silk fibroin/chitosan/nanohydroxyapatite core–shell nanofibrous membranes. ACS Appl Mater Interfaces 2015;7(38):21170–81.
[105] Chen H, Huang X, Zhang M, Damanik F, Baker MB, Leferink A, et al. Tailoring surface nanoroughness of electrospun scaffolds for skeletal tissue engineering. Acta Biomater 2017;59:82–93. Erratum in: Acta Biomater 2017; 71:525.